Article

Research on Temporal and Spatial Differentiation and Impact Paths of Agricultural Grey Water Footprints in the Yellow River Basin

Ruifan Xu [1], Jianwen Shi [2], Dequan Hao [1], Yun Ding [1] and Jianzhong Gao [1,*]

[1]   School of Economics and Management, Northwest A&F University, Yangling 712100, China
[2]   School of Economics and Finance, Xi'an Jiaotong University, Xi'an 710061, China
[*]   Correspondence: gaojianzhong2003@nwafu.edu.cn; Tel.: +86-152-9169-7070; Fax: +86-152-9169-7070

Abstract: The scientific evaluation of water pollution in the Yellow River Basin was directly related to the sustainable utilization of water resources and the green development of the agricultural economy in this region. In this study, we focused on the planting industry, and measured the agricultural grey water footprint of 73 prefecture-level cities in the Yellow River Basin from 2000 to 2019. We used spatial autocorrelation analysis to reveal temporal and spatial differentiation characteristics, and we used the path analysis method to study the factors influencing the temporal evolution and spatial distribution. Taking 2015 as the study period, the agricultural grey water footprint showed a trend of first rising and then falling. The values and growth rates of the agricultural grey water footprint in different regions were quite different. According to the natural breakpoint method, the agricultural grey water footprints were divided into low, middle, high, and very high groups. There were obvious spatial differences in the agricultural grey water footprints, and these differences gradually decreased. Generally, the H–L and the L–L types were dominant. From 2000 to 2019, most prefecture-level cities maintained the same transition changes as those in the neighboring regions. Crop yield, economic scale, population scale, urban and rural structure, and technological innovation were found to be the key elements of spatiotemporal variation in the agricultural grey water footprint.

Keywords: agricultural grey water footprint; spatial autocorrelation; path analysis; Yellow River Basin

1. Introduction

In 2022, Central Document No. 1 clearly proposes to "promote the green development in agriculture and rural areas, strengthen comprehensive efforts to control pollution from non-point agricultural sources, further reduce agricultural investment, strengthen the resource utilization of livestock and poultry manure, promote the scientific use and recycling of agricultural film, and develop agricultural evaluation of green development", which is a very important theoretical proposition. The Yellow River Basin is an important ecological barrier and food base in China, and it is also an important ecological barrier and economic zone [1]. However, it has a fragile ecological background, a high resource and environment load, insufficient economic development and low development quality, and it is also the area with the highest agricultural water pressure in China [2]. In September 2019, the Chinese government highlighted "ecological protection and high-quality development of the Yellow River Basin" as a major national strategy. In 2020, the grain output in the nine provinces and autonomous regions along the Yellow River was about 239 million tons, an increase of 2.14% over the previous year, accounting for about 35.6% of the national total. The GDP of the primary industry was about CNY 2.34 trillion, an increase of 11.96% over the previous year, accounting for about 30.1% of the country. However, prioritizing food security has led to the externalization of the environmental cost of water resources in the Yellow River Basin, coupled with the inherent spatial–temporal dislocation of water

resources. This has further aggravated the water resources shortage and water environment pollution, and severely restricted the green development of agriculture and rural areas in the Yellow River Basin [3,4]. According to the results of China's second survey of pollution sources, in 2017, chemical oxygen demand (COD), total nitrogen (TN), and total phosphorus (TP) emissions from agricultural sources and rural household sources accounted for 80.6%, 53.0%, and 74.1% of the total pollutants emissions in the Yellow River Basin, respectively. This was higher than the national averages of 85.90%, 10.21%, and 1.36%. Agricultural non-point source pollution is relatively serious [5]. Therefore, under the condition of ensuring the sustainable utilization of water resources and the green development of agriculture, it is of great significance to improve agricultural water quality and efficiency, which is firstly based on the scientific evaluation of the agricultural water environment.

As a method by which to measure the impact of human activities on the water resources systems, the water footprint comprehensively investigates the direct and indirect water use, water consumption, and pollution of consumers or producers. This mainly includes the blue, green, and grey water footprint, which has become a global research hotspot [6]. Among these, the grey water footprint refers to the amount of freshwater resources required to assimilate the pollutant loads discharged by the absorption products, based on the natural background concentration and the existing water environmental quality standards [7]. This method fully reflects the interaction between human economic activities and the water environment system, which is helpful for comprehensively and scientifically evaluating water pollution and achieving sustainable water use and green development [8]. Combining existing research, firstly, the grey water footprint measurement mainly focuses on the selection of key pollutants. Wickramasinghe et al. developed calibrated models and predicted the grey water footprint of eight pollutants [9]. Hong et al. selected nitrogen fertilizer as an agricultural pollution source and calculated the agricultural grey water footprint in the North China Plain from 2000 to 2016 [10]. Muratoglu evaluated the grey water footprint of 81 provinces and 25 watersheds in Turkey, using the tier-1 method and the high-resolution leachate runoff fraction [11]. Wu et al. calculated the agricultural grey water footprint under the inter-field test modes of conventional diffuse irrigation (CDI) and water-saving irrigation (WSI), by tracking the source of evapotranspiration and the migration process of various nitrogen and phosphorus pollutants [12]. Feng quantified China's grey water footprint from 2003 to 2018 based on four pollutants: chemical oxygen demand (COD), ammonia nitrogen (NH3-N), total nitrogen (TN) and total phosphorus (TP) [13]. Most of the agricultural grey water footprint involved in the above studies were focused on the pollution of the water environment caused by the excessive application of nitrogen fertilizer, and less consideration was given to the grey water footprint caused by compound fertilizer abuse. However, nitrogen was the main element in nitrogen fertilizer, for example, the nitrogen content of amide nitrogen was high, which was 46.7%. Not all nitrogen fertilizers had 100% nitrogen content. In addition, compound fertilizer also contained 30% nitrogen element, which would also cause pollution to underground water. Ignoring nitrogen element pollution caused by compound fertilizer application would lead to bias in the research results. Secondly, regarding the temporal–spatial characteristics of the grey water footprint, Xie et al. measured and analyzed the green, blue, and grey water footprints of pig feeding and pork production in China from 2004 to 2013 and their spatial and temporal evolution patterns. They concluded that, over time, the regions with higher grey water footprints generated by pig rearing began to shift southward [14]. Lin et al. analyzed the temporal and spatial distribution characteristics of the grey water footprint and the change trend of the gravity center in 31 provinces (cities and districts) of China during 1998–2016. This was on the basis of revealing the spatial evolution characteristics of the grey water footprint in China, as well as at the provincial level during 2003–2015 [15]. Li et al. adopted the ESDA (Exploratory Spatial Data Analysis) method to analyze the temporal and spatial evolution of blue water footprint and grey water footprint in the Haihe River Basin [16]. Ma et al. used the water footprint method to investigate the

dynamic evolution of agricultural water consumption from 2005 to 2015 in Zhangjiakou, an extremely water-scarce city which was divided into six ecological zones (I, II, III, IV, V, and VI) [17]. The above studies provide a new perspective for the scientific evaluation of regional water environmental pollution [18–20]. However, the above studies only involved the grey water footprint at the national and provincial level, and there were few scholars in the perspective of river basin, on the scale of the space of the city level difference of grey water footprint system analysis and in-depth exploration, however, the river basin as a special geographical unit, the space had features such as integrity, extents and differences, grey water footprint on the basin geographical unit of space law how to present, was in line with the basin, which was a special geographical unit features, this kind of research had important guiding significance for the sustainable development of water resources environment in the basin. Finally, regarding factors affecting water footprint, He and Xiang calculated the grey water footprint of pollutants diluted by the agricultural, industrial, and livestock sectors in Hunan Province from 2001 to 2015, and analyzed the influencing factors using the extended STIRPAT (Stochastic Impacts by Regression on Population, Affluence and Technology) model. The urbanization level, proportion of tertiary industry, proportion of secondary industry, per capita GDP, intensity of grey water footprint, and foreign direct investment were the main influencing factors of the grey water footprint [21]. Based on the MRIO model and combined with an improved grey water footprint calculation method, Li et al. studied the impact of regional trade on China's grey water footprint, and found that coexisting compounds had a greater impact on the grey water footprint, while the effect of inter-regional trade on improving China's grey water footprint was not significant [22]. Li et al. calculated the water footprint generated by rice planting in 30 provinces (cities and districts) in China from 1996 to 2015 and determined its spatio-temporal influencing factors, finding that average temperature (ATE), irrigation water coefficient (IWC) and fertilizer application amount in a sown area (FER) all positively affected the water footprint in time and space [23]. Wang et al. analyzed the factors influencing the agricultural water footprint across desert regions of northern China, from 2003 to 2017, and found that potential evapo-transpiration was the main influencing factor, which explained 20.4% of the variation in the agricultural water footprint [24]. Based on the quantification of the blue water footprint and the green water footprint of major food crop production in 11 cities of Shanxi Province from 2005 to 2014, Feng et al. analyzed the spatiotemporal variation and climate influencing factors in combination with agricultural and climate data and found that sunshine, temperature, and rainfall, among various climate factors, were the main driving factors of the crop production water footprint [25]. Cai et al. evaluated Chinese agricultural water footprints from 2000 to 2017 and analyzed the influencing factors, and found that GDP per capita, total investment in fixed assets, the income level of rural residents, the proportion of food grown, spray and drip irrigation technology, low-pressure pipe irrigation technology and seepage control irrigation technology had significant positive impacts on the agricultural water footprint. In contrast, the proportion of secondary and tertiary industries, social retail consumption, urbanization, technology expenditure, and the effective irrigation area proportion had a significant inhibitory effect [26]. Existing studies attach importance to the elaboration of econometric models, but the analysis of the action mechanism of influencing factors of grey water footprint is insufficient, and the persuasiveness needs to be strengthened. The above studies only conduct overall regression analysis based on all research samples to explore the main influencing factors, ignoring the heterogeneity of influencing factors in different regions, only discuss the various direct influencing factors of the water footprint; however, the influencing factors of the water footprint are various, including, but not limited to, meteorological factors, and agricultural production inputs, such as macro policies; additionally, the mixed and complex dynamic relationships between influencing factors have indirect effects on the water footprint. Therefore, ignoring indirect effects may lead to bias in research results. In order to overcome the defects in the above studies, this study proposes the following innovations: Firstly, when calculating the agricultural grey water footprints, the existing studies focus on the pollution of water environments caused

by excessive application of chemical fertilizers (mainly nitrogen fertilizers) in the planting industry, whereas this study also considers the agricultural grey water footprint caused by other kinds of chemical fertilizers (nitrogen fertilizers and compound fertilizers), and 46% of nitrogen fertilizer content and 30% of compound fertilizer content are considered as nitrogen pollution. Secondly, most of the existing studies on the temporal and spatial characteristics of the grey water footprint only involve the provincial level, but this study comprehensively analyzes the temporal and spatial characteristics of the grey water footprint of the Yellow River Basin at the municipal level. Finally, as for studies regarding the influencing factors of water footprints, the existing studies only discuss the direct effects of various influencing factors on the water footprint, whereas we study the indirect effects of various influencing factors on the water footprint on this basis.

The marginal contribution of this paper was mainly reflected in three aspects: First, the calculation idea of grey water footprint was improved. This study not only considered the pollution of the water environment caused by excessive application of chemical fertilizers (mainly nitrogen fertilizer), but also took into account the influence of other kinds of fertilizers (nitrogen fertilizer and compound fertilizer) on the agricultural grey water footprint, which was the inheritance and expansion of existing studies. Second, for the study of the grey water footprint, this paper further considered the influence of spatial interaction, that is, to explore the interaction between regions and expand the application of spatial econometric model in this field. Third, although there have been studies on influencing factors of the grey water footprint in the academic community, the Tobit model was mainly used to analyze the impact of various indicators. This study comprehensively discusses the direct and indirect impacts of various influencing factors on the water footprint, which made up for the blind spot of empirical analysis in this field. Based on this, we focused on the planting industry, and measured the agricultural grey water footprint of 73 prefecture-level cities in the Yellow River Basin from 2000 to 2019. We used spatial autocorrelation analysis to reveal temporal and spatial differentiation characteristics, and used the path analysis method to study the factors influencing the temporal evolution and spatial distribution. This article is arranged as follows: the second part is the research methods and data sources; the third part presents the empirical analysis, including calculating the agricultural grey water footprints of 73 prefecture-level cities in the Yellow River Basin from 2000 to 2019 (using the spatial autocorrelation analysis to reveal the spatial and temporal differentiation characteristics of the agricultural grey water footprint), using the path analysis to study the influencing factors of the temporal evolution and spatial distribution of the agricultural grey water footprint; and the fourth part discusses conclusions and recommendations.

2. Research Methods and Data Sources

2.1. Research Methods

2.1.1. Agricultural Grey Water Footprint

In this study, the agricultural grey water footprint (AWF_{grey}) only refers to the grey water footprint of the planting industry [27,28].

Regarding crop growth, a large number of chemical fertilizers and pesticides are applied in order to reduce plant diseases and insect pests of crops and soil fertility. Most of these enter the water environment at a fixed proportion (leaching rate) under the action of the precipitation or irrigation water, causing surface runoff and underground water pollution [29]. According to the common model of the Water Footprint Assessment Manual, the grey water footprint from the planting industry can be calculated based on the leaching of nitrogen into water caused by fertilizer application (including nitrogen fertilizers and compound fertilizers) [7,30,31]. In this study, we only considered the grey water footprint of nitrogen produced by nitrogen fertilizers and compound fertilizers in the calculation [32–34]. The specific calculation formula is as follows [35]:

$$WF_{grey,plant}(\text{TN}) = \frac{\alpha \times (APPl_n \times C_n + APPl_c \times C_c)}{C_{max} - C_{nat}} \tag{1}$$

In Equation (1), $WF_{grey,plant}(\text{TN})$ (m^3) is the grey water footprint of the planting industry and α (%) represents the leaching rate; 7% of nitrogen was selected as the leaching rate in this study according to previous studies [32,36]. *APPl* is defined the abbreviation of the word "Application". $APPl_n$ (kg) and $APPl_c$ (kg) represent the annual yield of nitrogen fertilizer and compound fertilizer, respectively [35]. C_n and C_c represent a nitrogen content of 46% and 30% in nitrogen fertilizer and compound fertilizer, respectively [35]. C_{max} (kg/m^3) represents the water quality standard concentration of the pollutant N element in chemical fertilizers required by Grade III of the Environmental Quality Standards for Surface Water in China (GB3838-2002), set at 0.001 kg/m^3 [14]. C_{nat} (kg/m^3) represents the natural background concentration of the pollutants N element in chemical fertilizers in the receiving water, which is usually defaulted to 0 kg/ m^3 [37,38].

2.1.2. Spatial Autocorrelation Analysis Method

Spatial autocorrelation is usually used to analyze the correlation level between the attribute eigenvalue of a unit in a certain region of space and the same attribute eigenvalue of the unit in its adjacent region, which can be divided into global and local spatial autocorrelation [39,40]. Global spatial autocorrelation mainly analyzes whether regions have spatial relevance on the whole level. Local spatial autocorrelation mainly studies whether there is local spatial aggregation with high or low values in specific regions, and specific indexes under the condition of regional autocorrelation as a whole [41].

(1)   Global spatial autocorrelation (global Moran's *I*)

Global spatial autocorrelation can be used to analyze whether the spatial distribution of a certain attribute characteristic value of a research object is correlated in the overall research area, and to then judge whether such a phenomenon exists aggregated in space [42]. The global Moran index is a commonly used spatial autocorrelation measure, and its definition is as follows [43,44]:

$$\text{Moran's } I = \frac{\sum_{i=1}^{n}\sum_{j \neq i}^{n} W_{ij} z_i z_j}{\sigma^2 \sum_{i=1}^{n}\sum_{j \neq i}^{n} W_{ij}} \tag{2}$$

$$= \frac{n \sum_{i=1}^{n}\sum_{j \neq i}^{n} W_{ij}(x_i - \overline{x})(x_j - \overline{x})}{\sum_{i=1}^{n}\sum_{j \neq i}^{n} W_{ij} \sum_{i=1}^{n}(x_i - \overline{x})^2} \tag{3}$$

In Equations (2) and (3), n is the number of regions in space; x_i is the AWF_{grey} of region i; x_j is the AWF_{grey} of region j; z_i is the standard transformation of x_i ($z_i = \frac{(x_i - \overline{x})}{\sigma}$); z_j is the standard transformation of x_j ($z_j = \frac{(x_j - \overline{x})}{\sigma}$; $\overline{x} = \frac{1}{n}\sum_{i=1}^{n} x_i$) [43]; and W_{ij} is a binary adjacency space weight matrix, representing the adjacency relationship of space objects [44]. When region i is adjacent to region j, $W_{ij} = 1$; otherwise, $W_{ij} = 0$, $\sigma^2 = \frac{1}{n}\sum_{i=1}^{n}(x_i - \overline{x})^2$ [45]. The value range of Moran's I statistic is between -1 and 1. When I is within $[0, 1]$, it indicates that there is spatial positive correlation. The closer the value is to 1, the higher the spatial correlation degree is. When I is within $[-1, 0]$, it indicates that there is a spatial negative correlation. The closer the value is to -1, the higher the spatial difference degree. When I is equal to 0, it means that the spatial distribution is random and there is no spatial correlation [46]. The significance test of the Moran index requires the use of a standardized Z statistic [47], and the calculation is as follows:

$$Z = \frac{I - E(I)}{\sqrt{VAR(I)}} \tag{4}$$

In Equation (4), $E(I)$ and $VAR(I)$ are the expectation and variance of Moran's index, respectively. The null hypothesis is that there is no spatial autocorrelation. When Z > 1.96 or Z < -1.96, it indicates that there is a significant spatial autocorrelation [47,48].

(2)   Local spatial autocorrelation (local Moran's *I*)

The global spatial autocorrelation analysis reveals the interdependence degree of spatial units on the whole level, ignoring the possible local instabilities [49]. Therefore, in the case of significant global autocorrelation results, a local spatial autocorrelation analysis method is introduced to characterize the spatial dependence and spatial heterogeneity of specific regions. It is defined as follows [50,51]:

$$I_i(d) = Z_i \sum_{j \neq i}^{n} W_{ij} Z_j \tag{5}$$

In Equation (5), $I_i(d)$ is positive, indicating that region i is a high (low) value region and its adjacent region is also a high (low) value region, that is, there is a spatial agglomeration of similar values. If $I_i(d)$ is negative, it indicates that region i is a high (low) value region and its adjacent region is a low (high) value region, that is, there is a spatial agglomeration of different values [52,53].

Both Moran scatter plots and LISA (Local Indicators of Spatial Association) agglomeration maps can reveal the local characteristics of the spatial distribution of the AWF_{grey} in the Yellow River Basin in a more intuitive way. In the Moran scatter plot, the AWF_{grey} of prefecture-level cities in the Yellow River Basin is divided into four types. These correspond to different local spatial associations by taking the horizontal and vertical coordinates of the AWF_{grey} of prefecture-level cities as the abscissa, the spatial lag value of the AWF_{grey} as the ordinate, and the average horizontal and vertical coordinates of the scattered points as the central coordinate. The first is H–H aggregation, which indicates that the prefecture-level cities have a high AWF_{grey}, and the surrounding prefecture-level cities also have a high AWF_{grey}. The second is H–L aggregation, which indicates that the prefecture-level cities have a high AWF_{grey}, but the surrounding prefecture-level cities have a lower AWF_{grey}. The third is L–L aggregation, which indicates that the prefecture-level cities have a low AWF_{grey} and the surrounding prefecture-level cities also have a low AWF_{grey}. The fourth is L–H aggregation, which indicates that the prefecture-level cities have a low AWF_{grey}, but the surrounding prefecture-level cities have a higher AWF_{grey}.

2.1.3. Spatial Transition Method

As the Moran scatter diagram cannot accurately quantify the degree of cohesion and transition of spatial correlation, the measurement method for the space–time transition proposed by Rey et al. was adopted to further explore the spatiotemporal transfer characteristics of the local spatial correlation types of the AWF_{grey} in the Yellow River Basin [54]. The specific types and descriptions of the spatiotemporal transitions are shown in Table 1.

Table 1. Types and descriptions of spatiotemporal transitions.

Transition Type	Description	Transition Form	Transition Type	Description	Transition Form
Type I	The displacement of this region when there is no jump in the neighboring property values	$HH_t \rightarrow LH_{t+1}$ $HL_t \rightarrow LL_{t+1}$ $LH_t \rightarrow HH_{t+1}$ $LL_t \rightarrow HL_{t+1}$	Type III	Neighboring attribute values and local area attribute values leap simultaneously	$HH_t \rightarrow LL_{t+1}$ $HL_t \rightarrow LH_{t+1}$ $LL_t \rightarrow HH_{t+1}$ $LH_t \rightarrow HL_{t+1}$
Type II	Leap of related space adjacent to the prefecture-level city	$HH_t \rightarrow HL_{t+1}$ $HL_t \rightarrow HH_{t+1}$ $LH_t \rightarrow LL_{t+1}$ $LL_t \rightarrow LH_{t+1}$	Type IV	The same level is maintained for both adjacent and local	$HH_t \rightarrow HH_{t+1}$ $HL_t \rightarrow HL_{t+1}$ $LH_t \rightarrow LH_{t+1}$ $LL_t \rightarrow LL_{t+1}$

The calculation method of spatial cohesion of the AWF_{grey} in prefecture-level cities is as follows [49]:

$$S_t = \frac{F_{0.t}}{n} \tag{6}$$

In Equation (6), S_t is the degree of spatial cohesion; $F_{0,t}$ represents the number of prefecture-level cities of transition type IV in the study period of t; and n is 73 prefecture-level cities. The value range of S_t is [0, 1]. The larger the value of S_t, the more significant the spatial pattern locking or path dependence of the AWF_{grey} in the Yellow River Basin, and the greater the transition resistance [55,56].

2.1.4. Path Analysis

Path analysis was first established by S. Wright, an American scholar, in 1921. It is used to analyze the linear relationship between multiple independent variables and dependent variables. The direct path coefficient, indirect path coefficient, and total path coefficient can be used to study the direct effect of independent variables on the dependent variables, and the indirect effect of other independent variables on the dependent variables [57]. Path analysis theory proves that the simple correlation coefficient (r_iY) between any independent variable X_i and the dependent variable Y is the direct path coefficient (P_iY) between X_i and Y, plus the indirect path coefficient ($r_{ij}P_jY$) of all X_i passing through X_j and Y. The indirect path coefficient of any independent variable X_i on Y is the correlation coefficient (r_{ij}) of X_i and X_j multiplied by the path coefficient (P_jY) [58,59]. The relation equation of each coefficient is as follows:

$$\begin{cases} P_1 + r_{12}P_2 + \cdots + r_{1k}P_k = r_{1y} \\ r_{21}P_1 + P_2 + \cdots + r_{2k}P_k = r_{2y} \\ \qquad\qquad \vdots \\ r_{k1}P_1 + r_{k2}P_2 + \cdots + P_k = r_{ky} \end{cases} \tag{7}$$

In Equation (7), r_{ij} is the simple correlation coefficient of factor x_i and factor x_j (Pearson's correlation coefficient); r_{iy} is the simple correlation coefficient of factor x_i and dependent variable Y, also known as the total influence of factor x_i on dependent variable Y; P_i is the direct path coefficient, representing the direct influence of factor x_i on dependent variable Y, which is obtained by solving multiple linear equations; $r_{iy}P_j$ is the indirect path coefficient, representing the indirect effect of x_i on dependent variable Y through x_i; and $r_{iy}P_i$ represents the total contribution of x_i to the dependent variable Y [60–62].

In order to analyze the explanatory power and interaction of different influencing factors on the spatial–temporal variation of the AWF_{grey} in the Yellow River Basin, and considering the scientificity and comprehensiveness of the selection of indicators as well as the comparability and availability of data combined with the relevant literature [63–66], 12 influencing factors were selected. These 12 factors included: population scale, X_1; economic scale, X_2; urban and rural structure, X_3; technological innovation, X_4; industrial structure, X_5; resource endowment, X_6; crop yield, X_7; planting structure, X_8; proportion of agricultural water use, X_9; fertilizer application intensity, X_{10}; pesticide application intensity, X_{11}; and agricultural film application intensity, X_{12}. Among these, the population size is represented by the number of permanent residents; the economic scale is represented by the ratio of agricultural GDP to the agricultural population; the urban–rural structure is represented by the ratio of the agricultural population to the permanent population; scientific and technological innovation is represented by the R&D expenditure intensity; industrial structure is represented by the ratio of GDP to total GDP; resource endowment is represented by the total amount of water resources; planting structure is represented by the ratio of the sown area of grain crops to the sown area of commercial crops; the proportion of agricultural water use is represented by the ratio of agricultural water consumption to total water consumption; the intensity of chemical fertilizer application is represented by the ratio of the pure amount of chemical fertilizer applied to the total sown area of crops; the intensity of pesticide application is represented by the ratio of the applied amount of pesticides to the total sown area of crops; and the intensity of agricultural film application is represented by the ratio of the application amount of agricultural film to the total sown area of crops.

2.2. Data Sources

For this study, 73 prefecture-level cities in 9 provinces and autonomous regions of the Yellow River Basin were selected as the study area (Figure 1), and the time range of the data was 2000–2019. The relevant data came from the "China Statistical Yearbook", the "China Agricultural Yearbook", the "China Rural Statistical Yearbook", the "Sixty Years of New China Statistical Data Compilation", the "China Environmental Statistical Yearbook", and the statistical yearbooks and statistical bulletins of various provinces and cities; the data of some missing years were supplemented by the mean of the sum of the values of adjacent years.
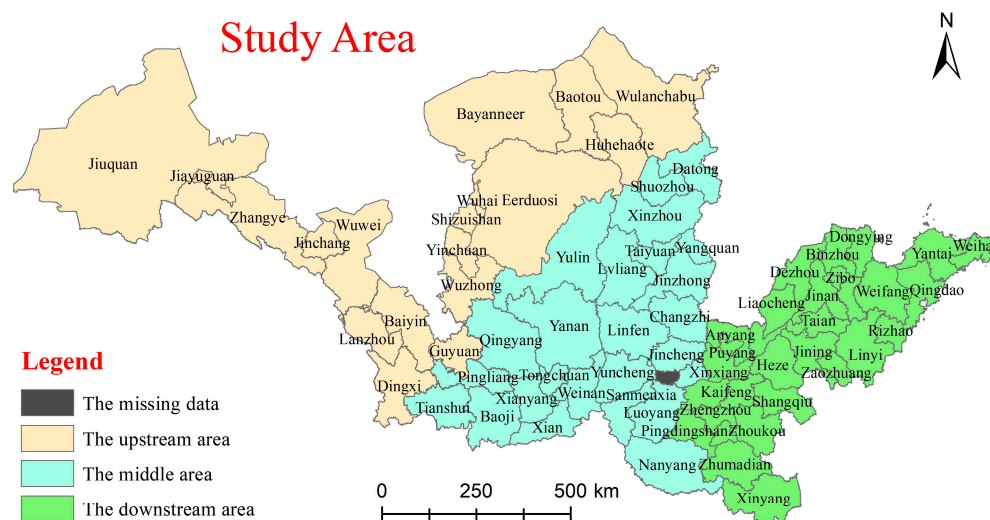

Figure 1. Study area map.

3. Results Analysis

3.1. Calculation Results of AWF_{grey}

On the whole, taking 2015 as the study period, the AWF_{grey} in the Yellow River Basin showed a trend of first rising and then falling (Figure 2). Among them, 2001−2006 was a period of rapid increase, where the average value of the AWF_{grey} increased sharply from 3.1×10^8 m^3 to 4.1×10^8 m^3, with an average annual growth rate of about 6.25%. From 2006 to 2015, it first decreased sharply and then increased slowly. The average AWF_{grey} first dropped sharply from 4.1×10^8 m^3 to 3.8×10^8 m^3 and then slowly climbed to 4.4×10^8 m^3, an increase of 0.6×10^8 m^3, with an average annual growth rate about 1.88%. From 2015 to 2019, there was a slow decline period. The average value of the AWF_{grey} decreased from 4.4×10^8 m^3 to 4.0×10^8 m^3, with an average annual reduction rate of about 2.12%.

From the perspective of changes in different sections of the basin (Figure 3), the initial level of the AWF_{grey} in the upper reaches of the Yellow River Basin was the lowest, and the multi−year average was stable at 1.4×10^8 m^3; the midstream regions were second, and the multi−year average was stable at 3.2×10^8 m^3; the downstream area was the highest, and the multi-year average was stable at 6.0×10^8 m^3, which is much larger than the sum of the AWF_{grey} in the middle and upper reaches. However, the AWF_{grey} in the upstream and midstream regions changed rapidly during the study period, with an average annual growth rate of about 2.39% and 2.28%, respectively, while the downstream region growth rate was only 1.27%. In 2006, the first pollution source census conducted in China found that the concentrations of pollutants such as COD MN and NH$_3$-N in the middle reaches of the Yellow River Basin were relatively high, and they flowed downstream along the river, resulting in serious downstream pollution. The region still has a long way to go in improving agricultural non-point source pollution.
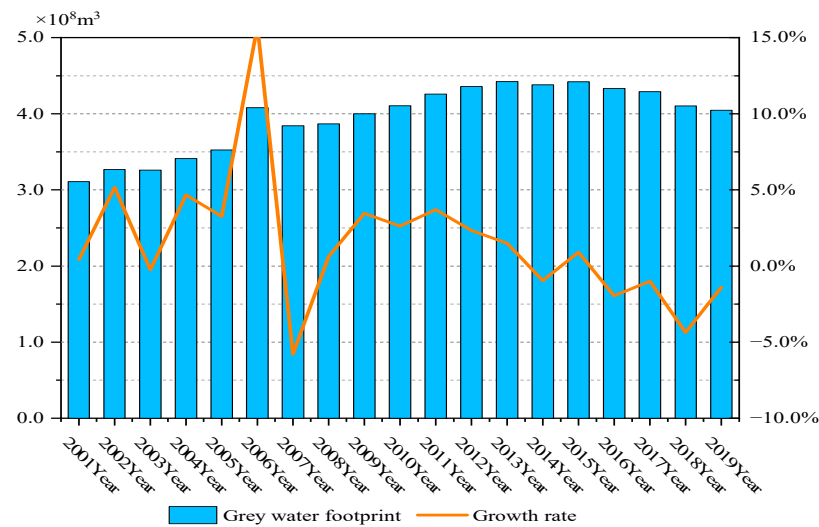
Figure 2. The overall evolution trend of AWF_{grey} in the Yellow River Basin.
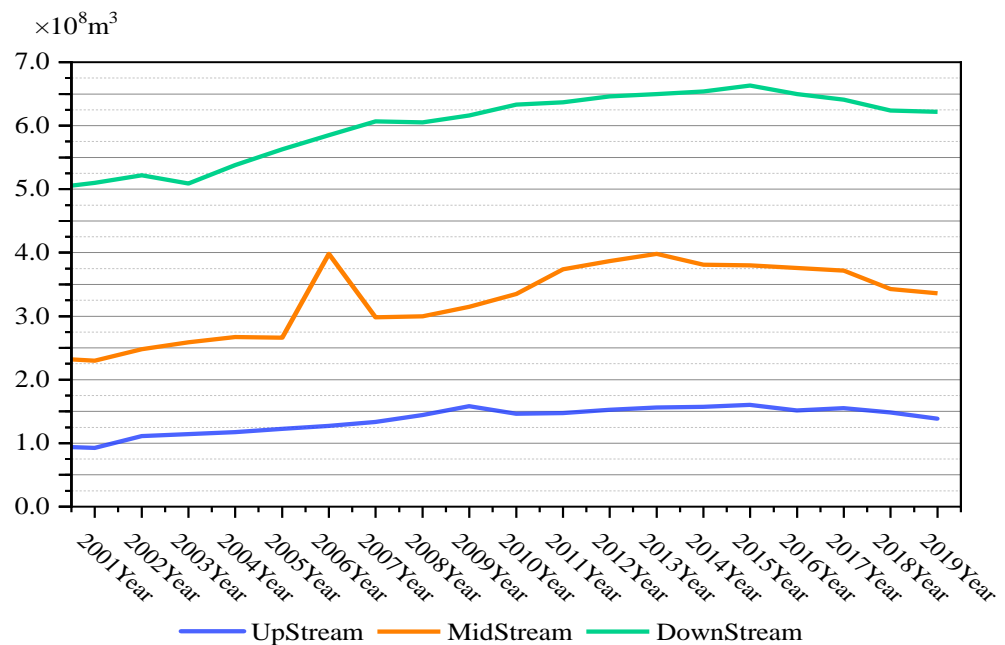

Figure 3. AWF_{grey} in the Upper, middle and lower Reaches of the Yellow River Basin from 2000 to 2019.

Further, based on the natural breakpoint method, the AWF_{grey} of prefecture-level cities in the Yellow River Basin from 2000 to 2019 is divided into four groups: low, medium, high, and very high. (Table 2). By drawing the spatial distribution map of the AWF_{grey} in the Yellow River Basin from 2000 to 2019 (Figure 4), it can be seen that, from 2000 to 2010, the overall spatial distribution pattern of the AWF_{grey} in the Yellow River Basin remained unchanged; however, the number of prefecture-level cities included in the low group and medium groups changed significantly. Specifically, the number of prefecture-level cities in the low group increased rapidly from 13 to 26, an increase of 100.00%; the number of prefecture-level cities in the middle group decreased from 27 to 16, a decrease of 40.74%; the number of prefecture-level cities in the high group decreased from 20 to 17, a decrease of 15.00%; and the number of prefecture-level cities in the very-high group increased from 13 to 14, an increase of 7.69%.

Table 2. Threshold ranges of AWF_{grey} in low, medium, high and very high groups (10^6 m^3).

Groups	2000	2010	2019
Low AWF_{grey} group	[2.2, 74.3]	[3.0, 169.9]	[0.63, 252.3]
Medium AWF_{grey} group	[74.3, 267.1]	[169.9, 371.8]	[252.3, 574.8]
High AWF_{grey} group	[267.1, 562.0]	[371.8, 725.7]	[574.8, 905.2]
Very high AWF_{grey} group	[562.0, 1038.9]	[725.7, 1399.9]	[905.2, 1579.0]

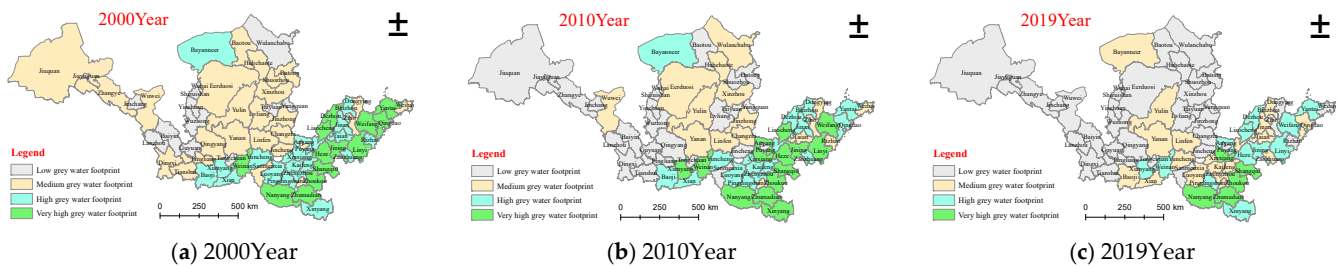(**a**) 2000Year (**b**) 2010Year (**c**) 2019Year

Figure 4. Spatial distribution of the AWF_{grey} in the Yellow River Basin from 2000 to 2019.

From 2010 to 2019, the overall spatial distribution pattern of the AWF_{grey} in the Yellow River Basin remained unchanged, but the number of prefecture-level cities included in the low and very-high groups changed significantly. Specifically, the number of prefecture-level cities in the low group increased rapidly from 26 to 36, an increase of 38.46%; the number of prefecture-level cities in the middle group increased from 16 to 19, an increase of 18.75%; the number of prefecture-level cities in the high group decreased from 17 to 13, a decrease of 23.53%; and the number of prefecture-level cities in the very high group decreased from 14 to 5, a decrease of 64.29%, indicating that the AWF_{grey} in the Yellow River Basin decreased significantly and the ecological environment improved significantly.

3.2. Spatial and Temporal Characteristics of the AWF_{grey} in the Yellow River Basin

This study calculated the global autocorrelation Moran's I index of the AWF_{grey} of cities in the Yellow River Basin from 2000 to 2019. Due to space limitations, only the global Moran's I index for 2000, 2010, and 2019 is shown (Figure 5). The AWF_{grey} of the Yellow River Basin has shown a significant positive correlation in the past 20 years, that is, the areas with a high AWF_{grey} are adjacent and the areas with a low AWF_{grey} are also adjacent, showing obvious spatial agglomeration. The value of Moran's I from 2000 to 2019 decreased slightly with the change in years, from 0.494 to 0.449, indicating that with the continuous development of the agricultural economy in the Yellow River Basin, the development speed of different regions has been inconsistent and the gap large. Therefore, the spatial agglomeration degree of the AWF_{grey} has been slightly weakened.

As the global Moran's I index is an overall autocorrelation statistic, which represents whether the elements are distributed with significant aggregation or separation at the overall level, it cannot reveal the spatial agglomeration degree of specific regions. The LISA agglomeration map is a clearer visual expression of the local Moran's I scatter plot. Analyzing the LISA agglomeration map can help to identify the "hot spot" and "blind spot" areas of the AWF_{grey} in the Yellow River Basin and intuitively represent the local characteristics of the AWF_{grey} in spatial distribution. Therefore, in this study, typical years were selected and LISA clustering maps were drawn for the AWF_{grey} for each prefecture-level city in the Yellow River Basin in 2000, 2010, and 2019 (Figure 6).

From 2000 to 2010, the number of prefecture-level cities with H–L agglomerations in the AWF_{grey} of the Yellow River Basin increased slightly, while the number of H–H, L–H, and L–L agglomerations decreased slightly. Specifically, the number of prefecture-level cities with H–L agglomeration increased from 38 to 47, an increase of 23.68%. The number of prefecture-level cities with H–H agglomeration decreased from 14 to 9, a decrease of 35.71%; the number of prefecture-level cities with L–H agglomeration decreased from 5 to

3, a decrease of 40.00%; and the number of prefecture- level cities with L–L agglomeration decreased from 15 to 13, a decrease of 13.33%.
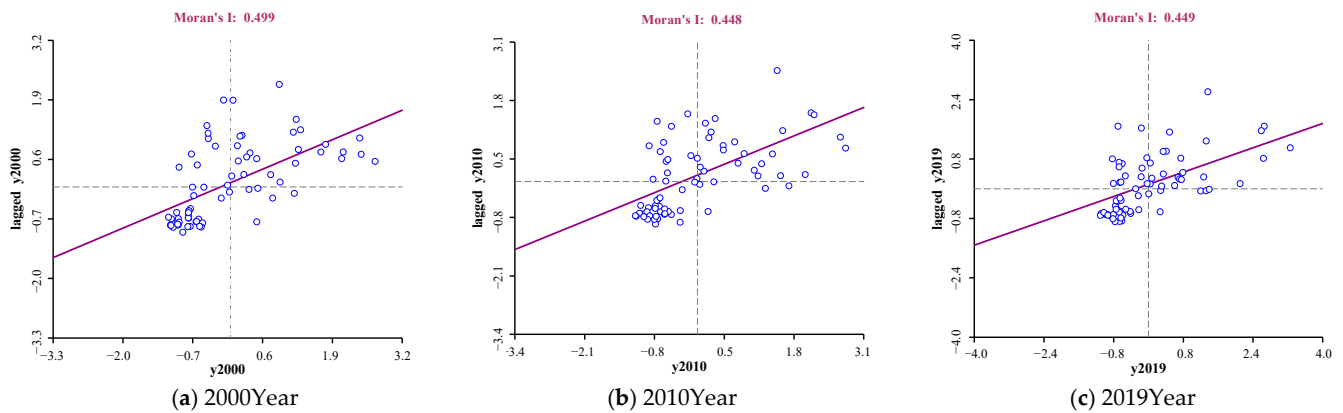

(**a**) 2000Year　　　　　　　　　　　(**b**) 2010Year　　　　　　　　　　　(**c**) 2019Year

Figure 5. Moran's index diagram of global autocorrelation of the AWF_{grey} of prefecture-level cities in the Yellow River Basin.

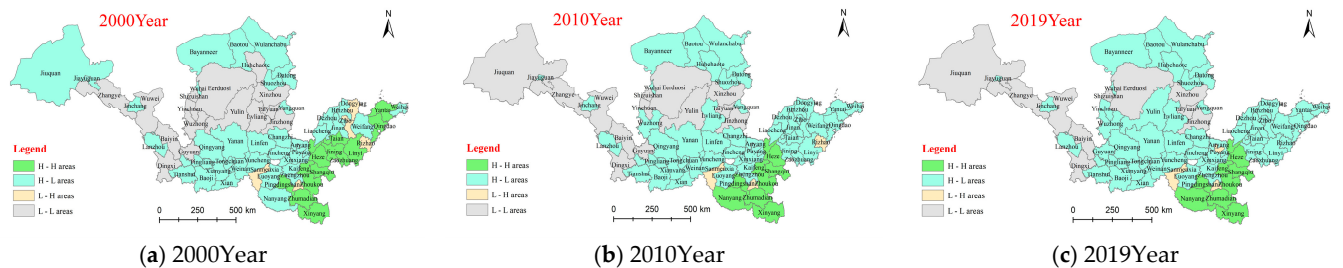(**a**) 2000Year　　　　　　　　　　　(**b**) 2010Year　　　　　　　　　　　(**c**) 2019Year

Figure 6. LISA agglomeration and distribution of the AWF_{grey} of prefecture-level cities in the Yellow River Basin from 2000 to 2019.

From 2010 to 2019, the number of prefecture-level cities with H–L agglomerations in the AWF_{grey} of the Yellow River Basin slightly increased; the number of H–H and L–H agglomerations remains the same; while the number of L–L agglomerations decreased slightly. Specifically, the number of H–L prefecture-level cities increased from 47 to 50, an increase of 6.38%; the number of prefecture-level cities with H–H agglomeration remained unchanged at 5; the number of prefecture-level cities with L–H agglomeration remained unchanged at 3; while the number of prefecture-level cities with L–L agglomeration decreased from 13 to 10, a decrease of 23.08%.

Further, by classifying the spatiotemporal transition types of the AWF_{grey} in 73 prefecture-level cities in the Yellow River Basin (Table 3), the most common transition type was generally transition type IV, that is, the AWF_{grey} of the spatial unit itself and the adjacent area maintained the same level of change. In the two time periods, the spatial cohesion increased from 81.94% to 93.06%, indicating that the spatial structure change of the AWF_{grey} in the Yellow River Basin has obvious path-dependent characteristics, and this characteristic is gradually strengthening. The next transition types are type II and type I, which reflect the influence of spatial proximity on the AWF_{grey} in some areas. Type III has the least transition in both the region itself and its adjacent areas. From 2000 to 2010, there were only two prefecture levels in Zibo and Dongying. Two prefecture-level cities, Hebi and Rizhao, appeared from 2010 to 2019, which further verified their atypical characteristics.

From 2000 to 2010, Jiuquan belonged to H–L agglomeration; influenced by the surrounding prefecture-level cities, it passively transitioned from H–L agglomeration to L–L agglomeration. Lvliang, Huhehaote, and Wuzhong all belonged to L–L agglomeration areas, and the AWF_{grey} was in a stable agglomeration state. Affected by their own AWF_{grey}, they took the initiative to transition from the original L–L agglomeration to H–L agglomeration.

Qingdao, Zaozhuang, Yantai, Jining, Taian, and Linyi all belonged to H–H agglomeration areas, and the AWF_{grey} was in a stable agglomeration state. Affected by their own AWF_{grey}, they took the initiative to transition from the original H–H agglomeration to H–L agglomeration. Nanyang belonged to H–L agglomeration; influenced by the surrounding prefecture-level cities, it passively transitioned from H–L agglomeration to H–H agglomeration. Zibo and Dongying all belonged to L–H agglomeration areas; influenced by the surrounding prefecture-level cities, they passively transitioned from L–H agglomeration to H–L agglomeration.

Table 3. LISA transition types of AWF_{grey} of 73 prefecture-level cities in the Yellow River Basin from 2000 to 2019.

Transition Type	Time Division	
	2000–2010	**2010–2019**
Type I	HL$_t$→LL$_{t+1}$: Jiuquan LL$_t$→HL$_{t+1}$: Lvliang, Huhehaote, Wuzhong	— LL$_t$→HL$_{t+1}$: Yulin, Yinchuan, Guyuan
Type II	HH$_t$→HL$_{t+1}$: Qingdao, Zaozhuang, Yantai, Jining, Taian, Linyi HL$_t$→HH$_{t+1}$: Nanyang	— —
Type III	— LH$_t$→HL$_{t+1}$: Zibo, Dongying	HL$_t$→LH$_{t+1}$: Hebi LH$_t$→HL$_{t+1}$: Rizhao
Type IV	The remaining 59 prefecture-level cities	The remaining 67 prefecture-level cities

From 2010 to 2019, Yulin, Yinchuan, and Guyuan all belonged to L–L agglomeration areas, and the AWF_{grey} was in a stable agglomeration state. Affected by their own AWF_{grey}, they took the initiative to transition from the original L–L agglomeration to H–L agglomeration. Hebei belonged to H–L agglomeration; influenced by the surrounding prefecture-level cities, it passively transitioned from H–L agglomeration to L–H agglomeration. Rizhao belonged to L–H agglomeration; influenced by the surrounding prefecture-level cities, it passively transitioned from L–H agglomeration to H–L agglomeration. In general, due to the different spatial correlation patterns of the AWF_{grey} in different cities, the spillover effect of inter-provincial AWF_{grey} may promote the convergence or differentiation of the AWF_{grey} in various regions, and then affect the overall structure of the AWF_{grey} spatial distribution in the Yellow River Basin.

3.3. Analysis of Influencing Factors of the AWF_{grey}

In this study, SPSS 27.0 (SPSS Inc., Chicago, IL, USA) was used to test the normal distribution of the spatiotemporal series data of the AWF_{grey} in the Yellow River Basin. Due to the small sample size, the results obtained by the Shapiro–Wilk Test were Sig = 0.275 and Sig = 0.266, which are both greater than 0.05 and obey normality. Therefore, the path analysis method could be used to study the temporal and spatial influencing factors of the AWF_{grey} in the Yellow River Basin. From 2000 to 2019, the analysis results of the influencing factors of the time series change of the AWF_{grey} in the Yellow River Basin are shown in Table 2. As the spatial distribution pattern of the AWF_{grey} in the Yellow River Basin was stable in different years, the dependent variable AWF_{grey} and the mean value of the independent variable from 2000 to 2019 were calculated to analyze the influencing factors of the spatial distribution of the AWF_{grey}.

It can be seen from Table 4 that the absolute values of the direct path coefficients of the factors affecting the time series changes of the AWF_{grey} in the Yellow River Basin are X_7, X_2, X_3, X_4, X_1, X_5, X_8, X_9, X_{10}, X_{11}, X_6, and X_{12}, indicating that crop yield, economic scale, and urban and rural structure have a great direct impact on the AWF_{grey}, and the direct path coefficients are 1.712, −0.537, and 0.310, respectively. However, the direct influence of pesticide application intensity, resource endowment, and agricultural film application intensity are small, and the direct path coefficients are 0.022, 0.021, and 0.018, respectively. Through the analysis of the indirect path coefficient between the influencing factors, it can be concluded that each influencing factor has a great impact on the AWF_{grey} according

to crop yield, economic scale, urban and rural structure, and technological innovation. In terms of crop yield, population scale has a strong positive impact on the increase in the AWF_{grey}, while industrial structure has a strong negative impact on the increase in the AWF_{grey} according to the crop yield. In terms of economic scale, the urban and rural structure has a strong positive impact on the increase in the AWF_{grey}, while population scale has a strong negative impact on the increase in the AWF_{grey} according to the economic scale. In terms of urban and rural structure, the industrial structure has a strong positive impact on the increase in the AWF_{grey}, while the economic scale has a strong negative impact on the increase in the AWF_{grey} according to the urban and rural structure. In terms of technological innovation, the urban and rural structure has a strong positive impact on the increase in the AWF_{grey}, while population scale has a strong negative impact on the increase in the AWF_{grey} according to the technological innovation. Industrial structure and crop yield have the largest total influence on the AWF_{grey}, with the total influence coefficients of -0.473 and 0.468, respectively.

Table 4. Analysis results of influencing factors of temporal variation of AWF_{grey} in the Yellow River Basin.

Influencing Factors	Direct Path Factor	Indirect Path Factor												Total Influence Factor
		X_1	X_2	X_3	X_4	X_5	X_6	X_7	X_8	X_9	X_{10}	X_{11}	X_{12}	
X_1	-0.191		-0.521	-0.302	-0.281	0.074	-0.008	1.625	-0.033	-0.029	-0.002	-0.005	-0.001	0.325
X_2	-0.537	-0.185		-0.307	-0.271	0.071	-0.007	1.583	-0.032	-0.028	-0.003	-0.006	-0.002	0.275
X_3	0.310	0.186	0.532		0.273	-0.074	0.007	-1.641	0.032	0.028	0.004	0.006	0.002	-0.335
X_4	-0.294	-0.183	-0.496	-0.288		0.072	-0.006	1.568	-0.032	-0.028	-0.001	-0.004	0.000	0.307
X_5	-0.079	0.178	0.485	0.292	0.267		0.006	-1.694	0.031	0.027	0.004	0.007	0.003	-0.473
X_6	0.021	0.076	0.175	0.106	0.089	-0.024		-0.663	0.016	0.015	-0.007	-0.006	-0.006	-0.207
X_7	1.712	-0.181	-0.497	-0.297	-0.269	0.078	-0.008		-0.032	-0.028	-0.003	-0.006	-0.002	0.468
X_8	-0.035	-0.181	-0.494	-0.284	-0.269	0.069	-0.010	1.544		-0.031	-0.003	-0.005	-0.002	0.299
X_9	-0.033	-0.168	-0.457	-0.261	-0.250	0.064	-0.010	1.430	-0.033		-0.003	-0.005	-0.002	0.271
X_{10}	0.023	0.020	0.077	0.047	0.014	-0.014	-0.007	-0.222	0.005	0.005		0.021	0.017	-0.012
X_{11}	0.022	0.042	0.137	0.084	0.049	-0.024	-0.006	-0.431	0.008	0.008	0.022		0.018	-0.068
X_{12}	0.018	0.014	0.055	0.037	0.007	-0.014	-0.007	-0.194	0.003	0.004	0.022	0.022		-0.032

It can be seen from Table 5 that the absolute values of the direct path coefficients of the factors affecting the spatial variation of the AWF_{grey} in the Yellow River Basin are X_4, X_1, X_7, X_{12}, X_6, X_3, X_9, X_5, X_{10}, X_8, X_{11}, and X_2, indicating that technological innovation, population size, and crop yield have a strong direct impact on the AWF_{grey}, with the direct path coefficients being 0.369, 0.355, and 0.284, respectively. However, the direct effects of planting structure, pesticide application intensity, and economic scale are relatively small, with the direct path coefficients being -0.057, 0.033, and -0.026, respectively. According to the analysis of the indirect path coefficients of the influencing factors, it can be concluded that each influencing factor has a strong impact on the AWF_{grey} according to economic scale, crop yield, population scale, and resource endowment. Among these, in terms of economic scale, crop yield has a strong positive impact on the increase in the AWF_{grey}, while planting structure has a strong negative impact on the increase in the AWF_{grey} according to the economic scale. In terms of crop yield, population scale has a strong positive impact on the increase in the AWF_{grey}, while planting structure has a strong negative impact on the increase in the AWF_{grey} according to the crop yield. In terms of population size, crop yield has a strong positive impact on the increase in the AWF_{grey}, while economic scale has a strong negative impact on the increase in the AWF_{grey} according to the population size. In terms of resource endowment, population size has a strong positive impact on the increase in the AWF_{grey}, while planting structure has a strong negative impact on the increase in the AWF_{grey} according to the resource endowment. Technological innovation, population size, and resource endowment have the largest total impact on the AWF_{grey}, with total impact coefficients of 0.949, 0.947, and 0.668, respectively.

Table 5. Analysis results of influencing factors of spatial variation of AWF_{grey} in the Yellow River Basin.

Influencing Factors	Direct Path Factor	Indirect Path Factor												Total Influence Factor
		X_1	X_2	X_3	X_4	X_5	X_6	X_7	X_8	X_9	X_{10}	X_{11}	X_{12}	
X_1	0.355		0.004	0.019	0.275	−0.018	0.054	0.245	0.007	−0.001	0.000	0.004	0.001	0.947
X_2	−0.026	−0.054		−0.029	0.041	0.003	−0.004	0.010	0.024	0.034	0.011	0.014	0.036	0.060
X_3	0.077	0.087	0.010		0.114	−0.046	0.025	0.089	0.002	−0.005	−0.014	−0.004	−0.011	0.323
X_4	0.369	0.265	−0.003	0.024		−0.035	0.041	0.247	0.015	0.009	0.004	0.003	0.010	0.949
X_5	−0.071	0.091	0.001	0.050	0.181		0.030	0.117	0.012	0.011	−0.012	−0.003	0.003	0.411
X_6	0.081	0.239	0.001	0.023	0.186	−0.026		0.151	0.009	0.007	−0.006	0.003	0.001	0.668
X_7	0.284	0.307	−0.001	0.024	0.321	−0.029	0.043		0.017	0.014	0.006	0.007	0.018	1.010
X_8	−0.057	−0.045	0.011	−0.003	−0.097	0.015	−0.012	−0.085		−0.061	−0.010	−0.011	−0.040	−0.395
X_9	−0.074	0.004	0.012	0.005	−0.046	0.011	−0.007	−0.055	−0.047		−0.007	−0.016	−0.049	−0.267
X_{10}	0.066	0.000	−0.004	−0.017	0.024	0.012	−0.007	0.024	0.009	0.007		0.006	0.007	0.128
X_{11}	0.033	0.048	−0.011	−0.010	0.030	0.007	0.006	0.057	0.020	0.035	0.013		0.055	0.284
X_{12}	0.103	0.005	−0.009	−0.008	0.035	−0.002	0.001	0.049	0.022	0.035	0.005	0.018		0.252

4. Conclusions and Suggestions

4.1. Conclusions

In order to provide a scientific decision-making basis for the sustainable utilization of water resources and green development of agriculture in the Yellow River Basin, the temporal and spatial variation characteristics and influencing paths of the agricultural grey water footprint were studied in this paper. The main conclusions are as follows:

(1) Based on the water footprint theory, the AWF_{grey} of the Yellow River Basin from 2000 to 2019 was calculated. Taking 2015 as the study period, the results showed that the AWF_{grey} of the Yellow River Basin had a trend of rising first and then falling. The values and growth rates of the AWF_{grey} in different regions were quite different. The downstream value was much higher than that of the middle and upper reaches, but the growth rate was lower than that of the middle and upper reaches. In terms of temporal variation, the thresholds of the low, medium, high, and very-high AWF_{grey} groups increased, while the proportion of prefecture-level cities in the high and very-high AWF_{grey} groups decreased. In terms of spatial distribution, the low-AWF_{grey} group was mainly concentrated in the upper and middle reaches, the middle-AWF_{grey} group was mainly concentrated in the middle and lower reaches, and the high- and very-high-AWF_{grey} groups were mainly concentrated in the lower reaches and gradually decreased over time.

(2) Based on the LISA agglomeration map, the spatial correlation characteristics of the AWF_{grey} of the cities in the Yellow River Basin were analyzed. The results showed that the distribution of the AWF_{grey} in the Yellow River Basin not only had continuity in time, but also had obvious spatial agglomeration, and this difference gradually decreased. Generally, the "High–Low" agglomeration and the "Low–Low" agglomeration were dominant. From 2000 to 2019, most prefecture-level cities maintained the same transition changes as the neighboring regions. In the two time periods, spatial cohesion increased from 81.94% to 93.06%, indicating that the spatial structure change of the AWF_{grey} in the Yellow River Basin had obvious path-dependent characteristics, and this characteristic was gradually strengthened.

(3) Based on the path analysis method, the influencing factors of AWF_{grey} spatial and temporal variation in the Yellow River Basin were analyzed. The results showed that crop yield, economic scale, and urban and rural structure were the main driving factors affecting the temporal variation of the AWF_{grey} in the Yellow River Basin, and their direct path coefficients were 1.712, −0.537, and −0.310, respectively. Technological innovation, population size, and crop yield were the main influencing factors affecting the spatial distribution pattern, and their direct path coefficients were 0.369, 0.355, and 0.284, respectively. Crop yield was the only common factor influencing the spatio-temporal evolution of the AWF_{grey} in the Yellow River Basin. Chen's research

holds that economic development and technological effects are the main negative and positive factors behind the decline in the grey water footprint, respectively [67]. In this study, economic scale was the main negative factor that leads to the increase in the agricultural grey water footprint. For the temporal change of the agricultural grey water footprint, scientific and technological innovation was the main negative factor that leads to the increase in the agricultural grey water footprint. Kong found that, according to the intensity and grey water footprint of Chinese provincial agriculture and the agricultural GDP, there was a growth inhibitory effect of the grey water footprint, and the driving role was determined [68]. In this study, we found the opposite conclusion in that economies of scale affected the main negative factors driving the temporal changes of the agricultural grey water footprint of the Yellow River. This may be caused by the study of the regional difference taking cities as the research object, so the scale was smaller and the results were more targeted.

4.2. Suggestions

Based on the above research conclusions, we proposed the following suggestions:

(1) Appropriately control the population and the scale of agricultural economic development in the areas along the Yellow River Basin, and achieve balanced development between urban and rural areas. On the one hand, for the regions with a large population, the government should issue corresponding subsidy policies for out-migrating workers based on the actual situation of the city, and encourage a large number of young people to work and do business in the eastern region. On the other hand, for the regions with a small population, the government should strengthen the construction of living facilities for the residents, improve the level of education and medical care, reduce the cost of living, and attract people from other provinces to settle in this area, in order to realize the overall development of urban and rural areas in the Yellow River Basin.

(2) Based on regional resource endowments, the layout of agricultural production should be optimized and the agricultural planting structure should be rationally adjusted to maximize the efficiency of grain output. Each region should build important agricultural production bases with distinctive advantages according to their regional resource endowments. Furthermore, the layout of agricultural production should be optimized and the agricultural planting structure should be rationally adjusted to maximize the scale efficiency of grain production, thereby reducing the agricultural grey water footprint, and accelerating the high-quality development of various agricultural regions.

(3) Rely on the progress of agricultural science and technology to develop environment-friendly agriculture. Specifically, it is necessary to call on all municipal agricultural technology centers to hold online training courses on chemical fertilizer and pesticide reduction and efficiency enhancement technologies to guide farmers on how to popularize and apply "soil testing and formula fertilization technology" according to the fertilizer requirements of different crops. In addition, the National Agricultural Technology Center can also conduct training courses in various cities to demonstrate the relevant techniques to farmers and encourage them to observe and communicate, so as to explore new technologies for reducing chemical fertilizers and pesticides.

While offering a new perspective on evaluating agricultural water environment pollution in the Yellow River Basin, our study has limitations that represent opportunities for further research. First, due to the current academic circles not having reached a unified view on the definition of or calculation methods for the total agricultural grey water footprint (including planting, livestock, poultry breeding, and aquaculture, as well as data limitations), when calculating the agricultural grey water footprint, we only considered the grey water footprint produced by the application of chemical fertilizers (nitrogen fertilizers and compound fertilizers) in the planting industry. This may lead to a conservative value of the calculated agricultural grey water footprint. Second, through an empirical analysis,

it was concluded that the agricultural grey water footprint of different regions in the Yellow River basin has differences in the spatial scale, but how does the spatial differences evolve? Will the gap in the agricultural grey water footprint of different regions converge over time? If so, what kind of convergence will it show? Due to the limitations of space and the focus of this paper, we have not yet discussed these issues yet. In the future, spatial convergence and other models will be introduced to further analyze these issues.

References

1. Fan, G.Q.; Zhang, D.Z.; Zhang, J.M.; Li, Z.; Sang, W.; Zhao, L.; Xu, M. Ecological environmental effects of Yellow River irrigation revealed by isotope and ion hydrochemistry in the Yinchuan Plain, Northwest China. *Ecol. Indic.* **2022**, *135*, 108574. [CrossRef]
2. Fang, L.N.; Yin, C.B.; Fang, Z.; Zhang, Y. The promotion path of high-quality development of agriculture in the Yellow River Basin. *Chin. J. Agric. Resour. Reg. Plan.* **2021**, *42*, 16–22.
3. Lu, C.P.; Ji, W.; Hou, M.C.; Ma, T.; Mao, J. Evaluation of efficiency and resilience of agricultural water resources system in the Yellow River Basin, China. *Agric. Water Manag.* **2022**, *266*, 107605. [CrossRef]
4. Zhang, N.N.; Su, X.L.; Zhou, Y.Z.; Niu, J.-P. Water resources carrying capacity evaluation of the Yellow River Basin based on EFAST weight algorithm. *J. Nat. Resour.* **2019**, *34*, 1759–1770. [CrossRef]
5. Tao, Y.; Xu, J.; Ren, H.J.; Guan, X.; You, L.; Wang, S. Spatiotemporal evolution of agricultural non-point source pollution and its influencing factors in the Yellow River Basin. *Trans. Chin. Soc. Agric. Eng.* **2021**, *37*, 257–264.
6. Ercin, A.E.; Aldaya, M.M.; Hoekstra, A.Y. Corporate Water Footprint Accounting and Impact Assessment: The Case of the Water Footprint of a Sugar-Containing Carbonated Beverage. *Water Resour. Manag.* **2011**, *25*, 721–741. [CrossRef]
7. Hoekstra, A.Y.; Chapagain, A.K.; Aldaya, M.M.; Mekonnen, M.M. *The Water Footprint Assessment Manual*; Science Press: Beijing, China, 2012.
8. Ren, Z.A.; Rong, J.R. Decoupling Relationship Between Utilization of Water Resource and Economic Growth in Anhui. *J. Heilonjiang Univ. Technol.* **2017**, *17*, 58–63.
9. Wickramasinghe, W.M.S.; Navaratne, C.M.; Dias, S.V. Building resilience on water quality management through grey water footprint approach: A case study from Sri Lanka. *Procedia Eng.* **2018**, *212*, 752–759. [CrossRef]
10. Hong, C.C.; Liu, M.C.; Zhang, Y.J.; Wu, L.Q. Analysis on the intensity and efficiency of agricultural grey water footprint in Beijing-Tianjin-Hebei Region under the perspective of spatial-temporal patten. *J. Hebei Agric. Univ.* **2021**, *44*, 128–135.
11. Muratoglu, A. Grey water footprint of agricultural production: An assessment based on nitrogen surplus and high-resolution leaching runoff fractions in Turkey. *Sci. Total Environ.* **2020**, *742*, 140553. [CrossRef] [PubMed]
12. Wu, M.Y.; Li, Y.Y.; Xiao, J.F.; Guo, X.; Cao, X. Blue, green, and grey water footprints assessment for paddy irrigation-drainage system. *J. Environ. Manag.* **2022**, *302*, 114116. [CrossRef] [PubMed]
13. Feng, H.Y.; Sun, F.Y.; Liu, Y.Y.; Zeng, P.; Deng, L.; Che, Y. Mapping multiple water pollutants across China using the grey water footprint. *Sci. Total Environ.* **2021**, *785*, 147255. [CrossRef]

14. Xie, D.; Zhuo, L.; Xie, P.X.; Liu, Y.; Feng, B.; Wu, P. Spatiotemporal variations and developments of water footprints of pig feeding and pork production in China (2004–2013). *Agric. Ecosyst. Environ.* **2020**, *297*, 106932. [CrossRef]

15. Lin, J.W.; Weng, L.Y.; Dai, Y.H. Study on spatial and temporal pattern of grey water footprint and its decoupling relationship in China. *Water Conserv. Sci. Technol. Econ.* **2019**, *25*, 14–21.

16. Li, C.H.; Xu, M.; Wang, X.; Tan, Q. Spatial analysis of dual-scale water stresses based on water footprint accounting in the Haihe River Basin, China. *Ecol. Indic.* **2018**, *92*, 254–267. [CrossRef]

17. Ma, W.J.; Meng, L.H.; Wei, F.L.; Opp, C.; Yang, D. Spatiotemporal variations of agricultural water footprint and socioeconomic matching evaluation from the perspective of ecological function zone. *Agric. Water Manag.* **2021**, *249*, 106803. [CrossRef]

18. Zhang, Y.; Tan, Q.; Zhang, T.Y.; Zhang, T.; Zhang, S. Sustainable agricultural water management incorporating inexact programming and salinization-related grey water footprint. *J. Contam. Hydrol.* **2022**, *247*, 103961. [CrossRef]

19. Jamshidi, S.; Imani, S.; Delavar, M. An approach to quantifying the grey water footprint of agricultural productions in basins with impaired environment. *J. Hydrol.* **2022**, *606*, 127458. [CrossRef]

20. Yang, Z.W.; Li, B.; Xia, R.; Ma, S.; Jia, R.; Ma, C.; Wang, L.; Chen, Y.; Bin, L. Understanding China's industrialization driven water pollution stress in 2002–2015—A multi-pollutant based net gray water footprint analysis. *J. Environ. Manag.* **2022**, *310*, 114735. [CrossRef]

21. He, Z.W.; Xiang, P.A. An Analysis of the Variations and Driving Factors of Grey Water Footprint in Hunan Province. *China Rural Water Hydropower* **2018**, *10*, 19–26.

22. Li, H.; Liang, S.; Liang, Y.H.; Li, K.; Qi, J.; Yang, X.; Feng, C.; Cai, Y.; Yang, Z. Multi-pollutant based grey water footprint of Chinese regions. *Resour. Conserv. Recycl.* **2021**, *164*, 105202. [CrossRef]

23. Li, X.C.; Chen, D.; Cao, X.; Luo, Z.; Webber, M. Assessing the components of, and factors influencing, paddy rice water footprint in China. *Agric. Water Manag.* **2020**, *229*, 105939. [CrossRef]

24. Wang, Z.Y.; Xu, D.Y.; Peng, D.L.; Zhang, Y. Quantifying the influences of natural and human factors on the water footprint of afforestation in desert regions of northern China. *Sci. Total Environ.* **2021**, *780*, 146577. [CrossRef] [PubMed]

25. Feng, B.B.; Liu, X.F.; Zhao, Y.G.; Li, K. Estimate of blue and green water footprint of crop production and analysis of its influencing factors in Shanxi province. *Res. Soil Water Conserv.* **2018**, *25*, 200–205, 214.

26. Cai, J.P.; Xie, R.; Wang, S.J.; Deng, Y.; Sun, D. Patterns and driving forces of the agricultural water footprint of Chinese cities. *Sci. Total Environ.* **2022**, *843*, 156725. [CrossRef] [PubMed]

27. Zhang, L.; Dong, H.J.; Geng, Y.; Francisco, M.J. China's provincial grey water footprint characteristic and driving forces. *Sci. Total Environ.* **2019**, *677*, 427–435. [CrossRef]

28. Hu, Y.; Huang, Y.; Tang, J.; Gao, B.; Yang, M.; Meng, F.; Cui, S. Evaluating agricultural grey water footprint with modeled nitrogen emission data. *Resour. Conserv. Recycl.* **2018**, *138*, 64–73. [CrossRef]

29. Corredor, J.A.G.; González, G.L.V.; Granados, M.V.; Gutiérrez, L.; Pérez, E.H. Use of the gray water footprint as an indicator of contamination caused by artisanal mining in Colombia. *Resour. Policy* **2021**, *73*, 102197. [CrossRef]

30. Liu, J.X.; Li, Y.; Zheng, Y.M.; Tong, S.; Zhang, X.; Zhao, Y.; Zheng, W.; Zhai, B.; Wang, Z.; Li, Z.; et al. The spatial and temporal distribution of nitrogen flow in the agricultural system and green development assessment of the Yellow River Basin. *Agric. Water Manag.* **2022**, *263*, 107425. [CrossRef]

31. Tsaboula, A.; Papadakis, E.N.; Vryzas, Z.; Kotopoulou, A.; Kintzikoglou, K.; Papadopoulou-Mourkidou, E. Assessment and management of pesticide pollution at a river basin level part I: Aquatic ecotoxicological quality indices. *Sci. Total Environ.* **2019**, *653*, 1597–1611. [CrossRef]

32. Chukalla, A.D.; Krol, M.S.; Hoekstra, A.Y. Grey water footprint reduction in irrigated crop production: Effect of nitrogen application rate, nitrogen form, tillage practice and irrigation strategy. *Hydrol. Earth Syst* **2018**, *20*, 3245–3259. [CrossRef]

33. Wang, S.Y.; Lin, Y.J. Spatial Evolution and its Drivers of Regional Agro-ecological Efficiency in China's from the Perspective of Water Footprint and Grey Water Footprint. *Sci. Geogr. Sin.* **2021**, *41*, 291–301.

34. Han, Q.; Sun, C.Z.; Zou, W. Grey water footprint efficiency measure and its driving pattern analysis on provincial scale in China from 1998 to 2012. *Resour. Sci.* **2016**, *38*, 1179–1191.

35. Wang, Y.Q.; Xian, C.F.; Ouyang, Z.Y. Integrated assessment of sustainability in urban water resources utilization in China based on grey water footprint. *Acta Ecol. Sin.* **2021**, *41*, 2983–2995.

36. Ju, X.T.; Xing, G.X.; Chen, X.P.; Zhang, S.L.; Zhang, L.J.; Liu, X.J.; Cui, Z.L.; Yin, B.; Christie, P.; Zhu, Z.L.; et al. Reducing environmental risk by improving N management in intensive Chinese agricultural systems. *Proc. Natl. Acad. Sci. USA* **2009**, *106*, 3041–3046. [CrossRef] [PubMed]

37. Mekonnen, M.M.; Hoekstra, A.Y. The green, blue and grey water footprint of crops and derived crop products. *Hydrol. Earth Syst.* **2011**, *15*, 1577–1600. [CrossRef]

38. De Girolamo, A.M.; Miscioscia, P.; Politi, T.; Barca, E. Improving grey water footprint assessment: Accounting for uncertainty. *Ecol. Indic.* **2019**, *102*, 822–833. [CrossRef]

39. Ma, F.C.; Liu, Q.N. Spatial Correlation Pattern and Influencing Factors of "Water Footprint Intensity of Grain Crops" in Heilongjiang Province. *Ecol. Econ.* **2021**, *37*, 121–127, 144.

40. Sun, L. *Spatial Empirical Study on Regional Differences and Influencing Factors of Water Footprint Intensity in China*; South China University of Technology: Guangzhou, China, 2017.

41. Kumari, M.; Sarma, K.; Sharma, R. Using Moran's I and GIS to study the spatial pattern of land surface temperature in relation to land use/cover around a thermal power plant in Singrauli district, Madhya Pradesh, India. *Remote Sens. Appl. Soc. Environ.* **2019**, *15*, 100239. [CrossRef]
42. Tepanosyan, G.; Sahakyan, L.; Zhang, C.S.; Saghatelyan, A. The application of Local Moran's I to identify spatial clusters and hot spots of Pb, Mo and Ti in urban soils of Yerevan. *Appl. Geochem.* **2019**, *104*, 116–123. [CrossRef]
43. Zhang, Y.Q.; Rashid, A.; Guo, S.S.; Jing, Y.; Zeng, Q.; Li, Y.; Adyari, B.; Yang, J.; Tang, L.; Yu, C.-P.; et al. Spatial autocorrelation and temporal variation of contaminants of emerging concern in a typical urbanizing river. *Water Res.* **2022**, *212*, 118120. [CrossRef] [PubMed]
44. Melecky, L. Spatial Autocorrelation Method for Local Analysis of the EU. *Procedia Econ. Financ.* **2015**, *23*, 1102–1109. [CrossRef]
45. Xiao, Y.X.; Gong, P. Removing spatial autocorrelation in urban scaling analysis. *Cities* **2022**, *124*, 103600. [CrossRef]
46. Hou, M.Y.; Yao, S.B. Convergence and differentiation characteristics on agro-ecological efficiency in China from a spatial perspective. *China Popul. Resour. Environ.* **2019**, *29*, 116–126.
47. Zhu, J.J.; Shi, X.Y. Analysis of Spatial Autocorrelation Patterns of Land Use and Influence Factors in Loess Hilly Region—A Case Study of Changhe Basin of Jincheng City. *Res. Soil Water Conserv.* **2018**, *25*, 234–241.
48. Meng, B.; Wang, J.F.; Zhang, W.Z. Evaluation of Regional Disparity in China Based on Spatial Analysis. *Sci. Geogr. Sin.* **2005**, *4*, 11–18.
49. Rey, S.J.; Janikas, M.V. Space-time analysis of regional systems. *Geogr. Anal.* **2006**, *38*, 67–86. [CrossRef]
50. Song, W.; Chen, Y. Selection of observed variables and measuring indicators for the land use spatial autocorrelation analysis. *J. Arid Land Resour. Environ.* **2015**, *29*, 37–42.
51. Ghalhari, G.F.; Roudbari, A.D. An investigation on thermal patterns in Iran based on spatial autocorrelation. *Theor. Appl. Clim.* **2018**, *131*, 865–876. [CrossRef]
52. Ren, H.R.; Shang, Y.J.; Zhang, S. Measuring the spatiotemporal variations of vegetation net primary productivity in Inner Mongolia using spatial autocorrelation. *Ecol. Indic.* **2020**, *112*, 106108. [CrossRef]
53. Lin, Z.; Chao, L.; Wu, C.Z.; Hong, W.; Hong, T.; Hu, X. Spatial analysis of carbon storage density of mid-subtropical forests using geostatistics: A case study in Jiangle County, southeast China. *Acta Geochim.* **2018**, *37*, 90–101. [CrossRef]
54. Cao, X.C.; Shao, G.C.; Wang, X.J.; Wang, Z.; He, X.; Yang, C. Generalized water efficiency and strategic implications for food security and water management: A case study of grain production in China. *Adv. Water Sci.* **2017**, *28*, 14–21.
55. Bi, D.D.; Wang, K.; Wang, L.J.; Fang, Y. Research on Industrial Eco-Efficiency and Spatio-Temporal Transition Characteristics of the Yangtze River Delta. *Econ. Geogr.* **2018**, *38*, 166–173.
56. Zhao, G.M.; Zhao, G.Q.; Chen, L.Z. Research on spatial and temporal evolution of carbon emission intensity and its transition mechanism in China. *China Popul. Resour. Environ.* **2017**, *27*, 84–93.
57. Tao, R.; Zhang, Q.Q.; Li, R.; Liu, T.; Chu, G.X. Response of roil N_2O emission to partial chemical fertilizer substituted by organic fertilizer in mulch-drip irrigated cotton field. *Trans. Chin. Soc. Agric. Mach.* **2015**, *46*, 204–211.
58. Cheng, W.T. *Economic Decoupling and Water Use Efficiency Analysis Based on Water Footprint of Farming in Liaoning Province*; Shenyang Agricultural University: Shenyang, China, 2020.
59. Zong, R.; Wang, Z.H.; Zhang, J.Z.; Li, W. The response of photosynthetic capacity and yield of cotton to various mulching practices under drip irrigation in Northwest China. *Agric. Water Manag.* **2021**, *249*, 106814. [CrossRef]
60. Yu, S.W.; Zhu, K.J.; Zhang, X. Energy demand projection of China using a path-coefficient analysis and PSO–GA approach. *Energy Convers. Manag.* **2012**, *53*, 142–153. [CrossRef]
61. Jia, L.J.; Fan, D.C.; Wu, Y.J. Research on industrial structural adjustment under the background of low carbon economy. *Inq. Into Econ. Issues* **2013**, *2*, 87–92.
62. Song, C.M.; Li, C.G.; Xiang, Y.L. Study on energy consumption's determinants based on path analysis. *J. Arid Land Resour. Environ.* **2012**, *26*, 174–179.
63. Li, Y.P.; Wu, W.N.; Yang, J.X.; Cheng, K.; Smith, P.; Sun, J.; Xu, X.; Yue, Q.; Pan, G. Exploring the environmental impact of crop production in China using a comprehensive footprint approach. *Sci. Total Environ.* **2022**, *824*, 153898. [CrossRef]
64. Zhao, J.C.; Han, T.; Wang, C.; Shi, X.; Wang, K.; Zhao, M.; Chen, F.; Chu, Q. Assessing variation and driving factors of the county-scale water footprint for soybean production in China. *Agric. Water Manag.* **2022**, *263*, 107469. [CrossRef]
65. Wang, Y.; Zhang, Y.H.; Sun, W.X.; Zhu, L. The impact of new urbanization and industrial structural changes on regional water stress based on water footprints. *Sustain. Cities Soc.* **2022**, *79*, 103686. [CrossRef]
66. Valis, D.; Hasilova, K.; Forbelska, M.; Pietrucha-Urbanik, K. Modelling water distribution network failures and deterioration. In Proceedings of the 2017 IEEE International Conference on Industrial Engineering and Engineering Management, Singapore, 10–13 December 2017; pp. 924–928. [CrossRef]
67. Chen, J.; Gao, Y.Y.; Qian, H.; Jia, H.; Zhang, Q. Insights into water sustainability from a grey water footprint perspective in an irrigated region of the Yellow River Basin. *J. Clean. Prod.* **2021**, *316*, 128329. [CrossRef]
68. Kong, Y.; He, W.J.; Zhang, Z.F.; Shen, J.; Yuan, L.; Gao, X.; An, M.; Ramsey, T.S. Spatial-temporal variation and driving factors decomposition of agricultural grey water footprint in China. *J. Environ. Manag.* **2022**, *318*, 115601. [CrossRef] [PubMed]